

Research article

CFD simulation of hydrothermal of a nanofluid in a microchannel subjected to a magnetic field

Mohammad Reza Assari^{1*}, Arman Mohammadian¹, Alireza Jafar Gholibeik¹

¹Department of Mechanical Engineering, Jundi-shapur University of Technology, Dezful, Iran

*assari@jsu.ac.ir

(Manuscript Received --- 08 Sep. 2021; Revised --- 14 Nov. 2021; Accepted --- 07 Dec. 2021)

Abstract

In this study, CFD simulation of hydrothermal of a nanofluid in a microchannel under a magnetic field with spherical depressions and protrusions on hot and cold walls is investigated. The effects of increasing Hartman (Ha) and Reynolds numbers (Re) in various volume fractions (ϕ) are investigated. The governing equation by using single-phase model, finite volume method, and SIMPLE algorithm are solved. Also, it assumes the flow is laminar, steady-state, and incompressible. The simulation is considered in ranges of $10 \leq Re \leq 150$, $0 \leq Ha \leq 10$, and $0 \leq \phi \leq 0.03$. The findings illustrate that in a certain Ha number, increasing in Re number and ϕ cause the Nu number increase. Also in a constant Re number, As the Ha number increases, the mean Nu number increases. Likewise, an increase in ϕ has enhanced heat transfer in all Re and Ha numbers. In a certain ϕ , as Ha number and Re number enhance the Nu number increases. By enhancing thermal conductivity, the heat transfer increases. When $Re=150$, the percentage increase of heat transfer in $\phi=0.03$ relative to pure fluid is %5.98.

Keywords: Magnetic field; Microchannel; Nanofluid; Numerical investigation; Heat transfer.

1-Introduction

There is growing evidence that dispersed nanoparticles in aqueous-based fluids have a significant effect on the effective thermal conductivity of nanofluids. Nanofluids are the suspension of nanoparticles in a base fluid. Suspended nanoparticles cause the fluid transfer properties to be completely altered and the heat transfer to be significantly improved. Due to these special properties, nanofluids are widely

used in heat transfer [1-3]. Mechanisms such as the use of magnetic fields increase heat transfer [4,5]. However, contradictory results have also been reported in this regard [6]. Ho et al. [7] numerically investigated the effects of temperature-variable thermophysical properties for water-aluminum oxide nanofluids in a tube. By applying a constant heat flux and assuming a laminar flow, they concluded that an increase in the concentration and

temperature of the nanofluid made the effects of temperature inlet and the thermophysical properties of the nanofluid on the Nusselt number more prominent. Dehghan et al. [8] analytically investigated the effect of temperature-variable thermal conductivity on the heat transfer of a fluid moving between two parallel plates. Using a constant heat flux and using the Darcy expansion, they concluded that a linear increase in the thermal conductivity of the porous material results in a semi-linear increase in the Nusselt number. Alipour et al. [9] in a 2-D microchannel, numerically studied the effect of tooth presence on the flow characteristics and gentle heat transfer of H₂O-Ag nanofluid in different volume fractions. Calculations were performed for two Re number values. It was found that the fluid has a higher temperature drop in the sections where it has teeth. That is, at the outlet of the microchannel, with increasing Re number and the presence of teeth and increasing the volume fraction, a greater temperature drop occurs. The presence of teeth in the microchannel increases the velocity and dimensionless temperature in the central line of the microchannel. Rashidi et al. [10] numerically studied the heat transfer of water-alumina nanofluid convection in a vertical channel with a sinusoidal wall under a magnetic field. They investigated the influence of nanoparticle volume fraction, sine wave amplitude, and Hartmann number on flow and heat transfer properties. Their findings demonstrated that with increasing Hartmann number, the velocity profile in the smooth channel and the velocity slope near the wall increase so that the vortices disappear near the wall. Nouri et al. [11] investigated the forced convection of a nanofluid under the influence of a

magnetic field in a sinusoidal channel. In that research, a magnetic field perpendicular to the channel was applied. Water was also used as the base fluid and copper as nanoparticles. Their results showed that at each wavelength of the channel, where the channel converges, the Nusselt number was increased due to the increased velocity near the walls. Also, at each channel wavelength, the volume fraction and the Hartmann number mainly affected the local Nusselt number. Javar et al. [12] numerically investigated the forced convection heat transfer of an iron-oxide nanofluid with a water-based fluid under the MHD. The geometry under study was a two-dimensional channel with a fixed lower temperature wall and an insulated upper wall, and a linear bipolar magnetic field was applied in the middle of the lower surface. In that research, the effect of different models of magnetic force in four different powers and Reynolds numbers 10, 25, 40 on heat transfer in single-phase and two-phase states was investigated. He concluded that the application of a magnetic field with each of the force models, at different scales, increases the heat transfer coefficient compared to the field-less state. Also, the single-phase method was predicted higher amounts of heat transfer than the two-phase method. In this article, the impact of Re and Ha numbers on the fluid flow and heat transfer of a nanofluid in a microchannel is investigated. In this paper, the results are reported in the form of graphs and contours.

2-Problem statement

Fig. 1 shows the two-dimensional geometry of the flow and the amplitude of the problem in a horizontal microchannel with spherical depressions and protrusions

on hot and cold walls in the presence of a magnetic field. In this study, in terms of boundary conditions, hot and cold walls, inlet and outlet areas, the area of application of the magnetic field, and how to place depressions and spherical protrusions on the walls are shown. The length and width of the microchannel are 0.02 m and 0.0015 m, respectively ($h = 0.1515$ and $L = 0.02$ m). Also, the width of each hot and cold microchannel wall is 0.00025 m and the width of the fluid area is 0.001 m. Calculations are performed by considering spherical depressions and protrusions in the upper and lower walls with a radius of 0.0005 m and a height of 0.00015 m from the microchannel floor. Water-based fluid and aluminum oxide powder (Al_2O_3) with a diameter of 30 nm with various volume fractions are used.

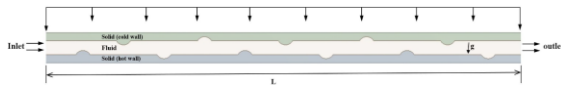


Fig. 1 Schematic of the present problem

3-Governing equations

The governing equations on the behavior of single-phase nanofluid flow by applying a uniform magnetic field, including the equations of, continuity, momentum, and energy in the Cartesian two-dimensional coordinate system, are as follows:

$$\frac{\partial u}{\partial x} + \frac{\partial v}{\partial y} = 0 \quad (1)$$

$$\rho_{nf} \left(u \frac{\partial u}{\partial x} + v \frac{\partial u}{\partial y} \right) = -\frac{\partial p}{\partial x} + \mu_{nf} \left(\frac{\partial^2 u}{\partial x^2} + \frac{\partial^2 u}{\partial y^2} \right) - \sigma_{nf} B_0^2 u \quad (2a)$$

$$\rho_{nf} \left(u \frac{\partial v}{\partial x} + v \frac{\partial v}{\partial y} \right) = -\frac{\partial p}{\partial y} + \mu_{nf} \left(\frac{\partial^2 v}{\partial x^2} + \frac{\partial^2 v}{\partial y^2} \right) \quad (2b)$$

$$(\rho C_p)_{nf} \left(u \frac{\partial T_{nf}}{\partial x} + v \frac{\partial T_{nf}}{\partial y} \right) = k_{nf} \left(\frac{\partial^2 T_{nf}}{\partial x^2} + \frac{\partial^2 T_{nf}}{\partial y^2} \right) \quad (3)$$

Eq. (4) is used to calculate the density of nanofluid [13],

$$\rho_{nf} = \phi \rho_p + (1 - \phi) \rho_f \quad (4)$$

To calculate the specific heat capacity of the nanofluid, constant and temperature-independent values and only a function of the volume fraction are proposed as follows [14],

$$(\rho C_p)_{nf} = \phi (\rho C_p)_p + (1 - \phi) (\rho C_p)_f \quad (5)$$

Eq. (6) is used to calculate the effective thermal conductivity of the nanofluid [15].

$$\frac{k_{nf}}{k_f} = 1 + 64.7 \phi^{0.7460} \left(\frac{d_f}{d_p} \right)^{0.3690} \left(\frac{k_p}{k_f} \right)^{0.7476} Pr^{0.9955} Re^{1.2321} \quad (6)$$

where:

$$Pr = \frac{\mu}{\rho_f \alpha_f}, \quad \mu = a \cdot 10^{\frac{b}{t-c}}, \quad \alpha_f = \frac{k_f}{\rho_f C_{p,f}}$$

$$a = 2.414e-5, \quad b = 247, \quad c = 140$$

$$Re = \frac{\rho_f \beta_c T}{3_\pi \mu^2 L_{bf}}, \quad L_{bf} = 0.17 \text{ nm}$$

$$\beta_c = 1.3807 \times 10^{-23}, \quad d_f = 0.1 \left(\frac{6m}{N \pi \rho_f} \right)^{\frac{1}{3}}$$

$$N = 6.022 \times 10^{23}$$

To calculate the effective dynamic viscosity of nanofluids, equation (7) is used [16],

$$\mu_{nf} = \frac{\mu_{bf}}{(1-\phi)^{2.5}} \quad (7)$$

Equation (8) is used to calculate the thermal diffusion coefficient of nanofluid,

$$\alpha_{nf} = \frac{k_{nf}}{(\rho C_p)_{nf}} \quad (8)$$

Equation (9) is used to calculate the electrical conductivity of nanofluids [17],

$$\sigma_{nf} = \sigma_f \left[1 + \frac{3 \left(\frac{\sigma_s}{\sigma_f} - 1 \right) \phi}{\left(\frac{\sigma_s}{\sigma_f} + 2 \right) - \left(\frac{\sigma_s}{\sigma_f} - 1 \right) \phi} \right] \quad (9)$$

The local convective heat transfer coefficient is calculated as follows,

$$h(x) = \frac{q''(x)}{T_w - T_b(x)} \quad (10)$$

The bulk temperature is calculated as follows [18,21],

$$T_b(x) = \frac{\int T \rho \vec{u} \cdot d\vec{A}}{\int \rho \vec{u} \cdot d\vec{A}} \quad (11)$$

To determine the amount of heat transfer from a heated surface to the fluid in contact with it, the Nusselt number is used. Having the value of heat transfer coefficient, the local Nusselt number is obtained as follows [19],

$$Nu(x) = \frac{h(x) D_h}{k_{nf}} \quad (12)$$

The mean Nusselt number is defined as follows,

$$Nu_{ave} = \int Nu(x) dx \quad (13)$$

The hydraulic diameter of the channel, which is one of the physical characteristics of the channel, is defined as follows:

$$D_h = \frac{4A_c}{p} \quad (14)$$

4-Validation

Since the two main keys in this research, nanofluid and magnetic field, are uniform, in this section, to ensure the numerical solution method, the validation of the present work with reference results [20] is used. Karimipour et al. [20] investigated fluid flow and heat transfer of water/carbon nanotube (FMWNT) in a rectangular microchannel under a uniform magnetic field. In their work, the lower wall of the microchannel was considered as insulation and the upper wall was divided into two parts. In one part of the upper wall, a constant heat flux with a uniform magnetic field was applied and in the other part, thermal insulation was considered. Fig. 2 shows the dimensionless horizontal velocity profiles on the centerline of the geometry in Hartmann numbers 0, 20, 40, and nanofluid with a volume fraction of 0.2% for Reynolds 10), which shows that the results are in good agreement with the numerical reference.

5-Results and discussion

Fig. 3 illustrates the mean Nu number diagram in terms of Re number for various ϕ and Ha numbers of zero and 10. According to the figure, heat transfer increases with increasing Re number in a Ha number and constant volume fraction. Also, by enhancing the thermal conductivity and increasing the Ha number in a certain Re number, the mean Nu number increases.

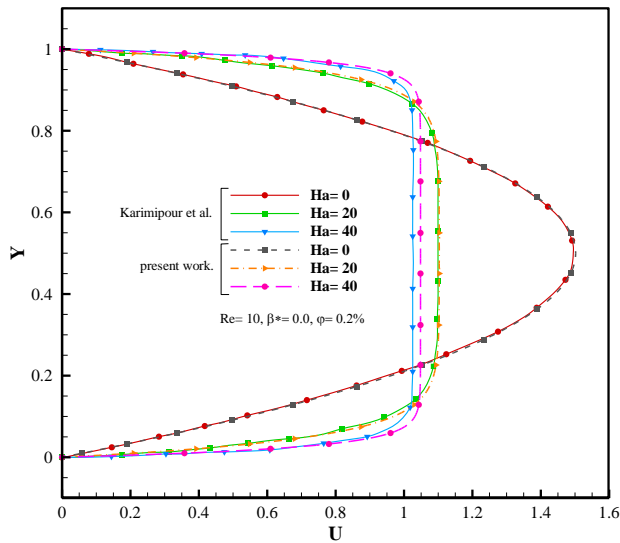


Fig. 2 Comparison of validation results with reference [20].

For a volume fraction of 3% and a Hartmann number of 0, the percentage increase of the mean Nusselt with $Re=150$ compared to nanofluid with $Re=10$ is 108.02%. Also, for the volume fraction of 3% and Hartmann number of 10, the increment of the mean Nu number with $Re=150$ compared to nanofluid with $Re=10$ is 126.70%. For $Re=150$ without field application, the increment of the mean Nu number with an $\phi=2\%$ compared to nanofluid with an $\phi=0\%$ is 5.30%. In addition, in this case, the increment of the mean Nu number with an $\phi=3\%$ compared to nanofluid with an $\phi=0\%$ is 7.07%. For $Re=150$ and $Ha=10$, the increment of the mean Nu number with an $\phi=1\%$ compared to nanofluid with an $\phi=0\%$ is 2.81% and the increment of the mean Nu number with an $\phi=2\%$ compared to nanofluid with an $\phi=0\%$ is 4.57% and finally, the increment of the mean Nu number with an $\phi=3\%$ compared to nanofluid with a $\phi=0\%$ is 5.97%. The comparison of the increment of the mean Nusselt with the $Re=150$ and the $\phi=3\%$ in the two Hartmann numbers of zero and 10 is 10.64%. The greatest effect of the Hartmann number on heat transfer is

in $Re=150$ and $Ha=10$ with a volume fraction of 3%.

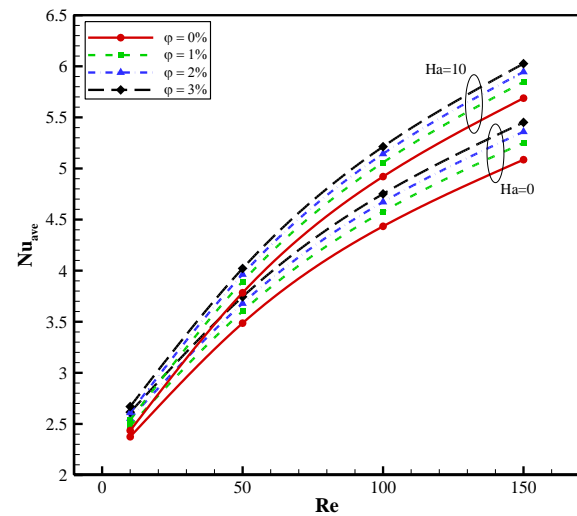


Fig. 3 The mean Nu number in terms of Re number for various ϕ and Ha numbers of zero and 10

To investigate the effect of magnetic field and Reynolds number on the dimensionless velocity profile, in Fig. 4, the dimensionless velocity profile in the vertical section of the channel at $x = 0.019$ m for a volume fraction of 3% nanoparticles in Hartmann numbers of 0, 5 and 10 for the flow is denoted by the $Re=150$. As can be seen, with increasing Hartmann number, the fluid velocity decreases due to the presence of Lorentz force in the opposite direction of the flow and the low momentum resistance of the fluid against it. According to Fig. 4, in the case without applying the magnetic field ($Ha=0$), due to the lack of Lorentz force, the velocity profile has reached its maximum value, but in the case of applying the magnetic field, due to the Lorentz force, the fluid velocity is reduced. As the field intensifies, this deceleration increases.

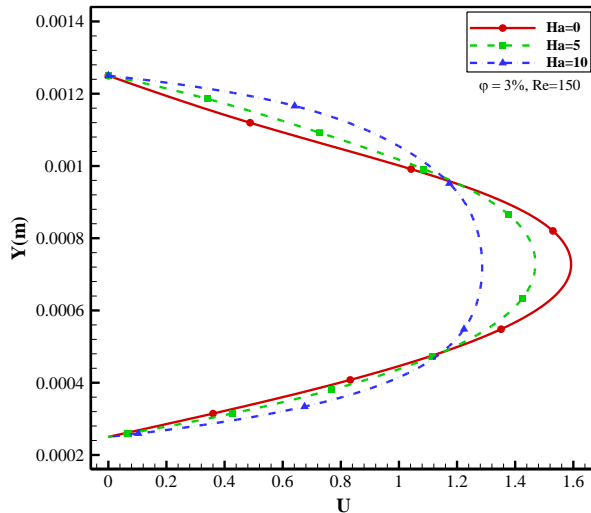


Fig. 4 Velocity profile in the vertical section of the channel at $x = 0.019$ for a volume fraction of 3% with a Reynolds number of 150 in different Hartmann numbers

Fig. 5 shows the velocity contour (left) and the temperature contour (right) at a $Re=10$ in the absence of a magnetic field. Development within the microchannel is quite evident. It can be seen that in the depressions, the fluid is trapped and the minimum flow velocity is observed. The maximum flow velocity is evident in the center of the microchannel. The temperature distribution inside the microchannel is more uniform at the output and the walls are completely affected by the applied boundary conditions.

6-Conclusion

In this paper, fluid flow and heat transfer in a microchannel under a magnetic field were investigated, the results of which can be obtained as follows:

- As the velocity increases, the Nu number enhances.
- As the ϕ increases, the Nu number enhances.

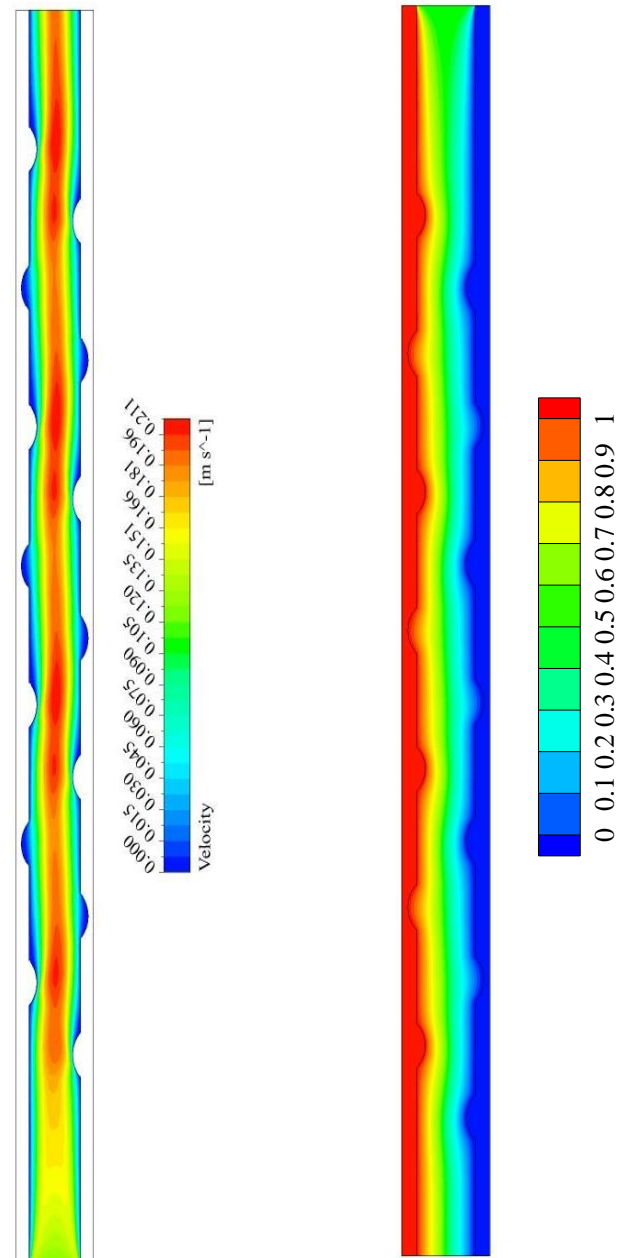


Fig. 5 Velocity contour (left) and the temperature contour (right) at a $Re=10$ under the absence of the MHD.

- The impact of the MHD has a positive effect on increasing heat transfer.
- The presence of MHD reduces the velocity peak and intensifies the velocity gradients adjacent to the wall.

References

- [1] Shahsavari, A., Noori, S., Toghraie, D., & Barnoon, P. (2021). Free convection of non-Newtonian nanofluid flow inside an eccentric annulus from the point of view of first-law and second-law of thermodynamics. *ZAMM-Journal of Applied Mathematics and Mechanics/Zeitschrift für Angewandte Mathematik und Mechanik*, 101(5), e202000266.
- [2] El-Shorbagy, M. A., Eslami, F., Ibrahim, M., Barnoon, P., Xia, W. F., & Toghraie, D. (2021). Numerical investigation of mixed convection of nanofluid flow in a trapezoidal channel with different aspect ratios in the presence of porous medium. *Case Studies in Thermal Engineering*, 25, 100977.
- [3] Monfared, R. H., Niknejadi, M., Toghraie, D., & Barnoon, P. (2021). Numerical investigation of swirling flow and heat transfer of a nanofluid in a tube with helical ribs using a two-phase model. *Journal of Thermal Analysis and Calorimetry*, 1-14.
- [4] Barnoon, P., Toghraie, D., Eslami, F., & Mehmandoust, B. (2019). Entropy generation analysis of different nanofluid flows in the space between two concentric horizontal pipes in the presence of magnetic field: single-phase and two-phase approaches. *Computers & Mathematics with Applications*, 77(3), 662-692.
- [5] Barnoon, P., & Ashkiyan, M. (2020). Magnetic field generation due to the microwaves by an antenna connected to a power supply to destroy damaged tissue in the liver considering heat control. *Journal of Magnetism and Magnetic Materials*, 513, 167245.
- [6] Barnoon, P., Toghraie, D., Salarnia, M., & Karimipour, A. (2020). Mixed thermomagnetic convection of ferrofluid in a porous cavity equipped with rotating cylinders: LTE and LTNE models. *Journal of Thermal Analysis and Calorimetry*, 1-40.
- [7] Ho, C. J., Chang, C. Y., Cheng, C. Y., Cheng, S. J., Guo, Y. W., Hsu, S. T., & Yan, W. M. (2016). Laminar forced convection effectiveness of Al₂O₃-water nanofluid flow in a circular tube at various operation temperatures: Effects of temperature-dependent properties. *International Journal of Heat and Mass Transfer*, 100, 464-481.
- [8] Dehghan, M., Valipour, M. S., & Saedodin, S. (2015). Temperature-dependent conductivity in forced convection of heat exchangers filled with porous media: a perturbation solution. *Energy Conversion and Management*, 91, 259-266.
- [9] Gravndyan, Q., Akbari, O. A., Toghraie, D., Marzban, A., Mashayekhi, R., Karimi, R., & Pourfattah, F. (2017). The effect of aspect ratios of rib on the heat transfer and laminar water/TiO₂ nanofluid flow in a two-dimensional rectangular microchannel. *Journal of Molecular Liquids*, 236, 254-265.
- [10] Rashidi, M. M., Nasiri, M., Khezerloo, M., & Laraqi, N. (2016). Numerical investigation of magnetic field effect on mixed convection heat transfer of nanofluid in a channel with sinusoidal walls. *Journal of Magnetism and Magnetic Materials*, 401, 159-168.
- [11] Nouri, R., Gorji-Bandpy, M., & Domiri Ganji, D. (2014). Numerical investigation of magnetic field effect on forced convection heat transfer of

nanofluid in a sinusoidal channel. *Modares Mechanical Engineering*, 13(14), 43-55.

[12] Ahmadi, A. A., Khodabandeh, E., Moghadasi, H., Malekian, N., Akbari, O. A., & Bahiraei, M. (2018). Numerical study of flow and heat transfer of water- Al_2O_3 nanofluid inside a channel with an inner cylinder using Eulerian–Lagrangian approach. *Journal of Thermal Analysis and Calorimetry*, 132(1), 651-665.

[13] Pak, B. C., & Cho, Y. I. (1998). Hydrodynamic and heat transfer study of dispersed fluids with submicron metallic oxide particles. *Experimental Heat Transfer an International Journal*, 11(2), 151-170.

[14] Xuan, Y., & Roetzel, W. (2000). Conceptions for heat transfer correlation of nanofluids. *International Journal of heat and Mass transfer*, 43(19), 3701-3707.

[15] Chon, C. H., Kihm, K. D., Lee, S. P., & Choi, S. U. (2005). Empirical correlation finding the role of temperature and particle size for nanofluid (Al_2O_3) thermal conductivity enhancement. *Applied Physics Letters*, 87(15), 153107.

[16] Brinkman, H. C. (1952). The viscosity of concentrated suspensions and solutions. *The Journal of chemical physics*, 20(4), 571-571.

[17] Barnoon, P., Toghraie, D., & Karimipour, A. (2020). Application of rotating circular obstacles in improving ferrofluid heat transfer in an enclosure saturated with porous medium subjected to a magnetic field. *Journal of Thermal Analysis and Calorimetry*, 1-23.

[18] Barnoon, P., Ashkiyan, M., & Toghraie, D. (2021). Embedding multiple conical vanes inside a circular porous channel filled by two-phase nanofluid to

improve thermal performance considering entropy generation. *International Communications in Heat and Mass Transfer*, 124, 105209.

[19] Barnoon, P., Toghraie, D., Mehmandoust, B., Fazilati, M. A., & Eftekhari, S. A. (2021). Comprehensive study on hydrogen production via propane steam reforming inside a reactor. *Energy Reports*, 7, 929-941.

[20] Karimipour, A., Taghipour, A., & Malvandi, A. (2016). Developing the laminar MHD forced convection flow of water/FMWNT carbon nanotubes in a microchannel imposed the uniform heat flux. *Journal of Magnetism and Magnetic Materials*, 419, 420-428.

[21] Barnoon, P., & Bakhshandehfard, F. (2021). Thermal management in biological tissue in order to degrade tissue under local heating process. *Case Studies in Thermal Engineering*, 101105.